International Journal of Pharmaceutics 358 (2008) 214–218

Contents lists available at ScienceDirect

International Journal of Pharmaceutics

journal homepage: www.elsevier.com/locate/ijpharm

Electronic structure and UV spectrum of fenofibrate in solutions

Yuan Le [a], Jian-Feng Chen [a,b,*], Min Pu [c]

[a] Key Laboratory for Nanomaterials, Ministry of Education, Beijing University of Chemical Technology, Beijing 100029, PR China
[b] Research Center of the Ministry of Education for High Gravity Engineering and Technology, Beijing University of Chemical Technology, Beijing 100029, PR China
[c] Education Ministry Key Laboratory of Science and Technology of Controllable Chemical Reaction, Beijing University of Chemical Technology, Beijing 100029, PR China

ARTICLE INFO

Article history:
Received 29 September 2007
Received in revised form 24 January 2008
Accepted 10 March 2008
Available online 29 March 2008

Keywords:
Fenofibrate
Solvent effects
Electronic structure
Excited states
UV absorption

ABSTRACT

The structure and UV spectra of fenofibrate have been evaluated in gas phase and in solutions using time dependent density functional theory (TDDFT) method at the B3LYP/6-31G(d), B3LYP/6-311G(d,p) and B3LYP/6-311++G(d,p) levels. The solvent effects have been taken into account based on the polarizable continuum model (PCM). The computed results appear that the introduction of dielectric medium has slight effect on the molecular geometry of fenofibrate. There is one allowed excited state presenting the strongest oscillator strength in the UV region, which is associated with the HOMO → LUMO and HOMO-1 → LUMO transition both in gas phase and in solutions. The prediction of the λ_{max} in THF, ethanol and DMSO is 285 nm, 286 nm and 287 nm, respectively, which are in a good agreement with experimental data of 284 nm, 285 nm and 288 nm.The results demonstrate that TDDFT-PCM is a useful tool for study of the electronic absorption in solutions.

1. Introduction

Fenofibrate, an oral fibrate lipid lowering agent, could markedly reduce elevated plasma concentrations of triglycerides. It also decreases elevated plasma concentrations of LDL and total cholesterol (Shi et al., 2005; Chong and Bachenheimer, 2000; Milionis et al., 2000). However, it is virtually insoluble in water, which adversely affects bioavailability. Recently, many processes have been designed to reduce the particle size in order to expand the surface area of drug exposed to the dissolution medium and thereby increase bioavailability. Most of these processes take place in a condensed medium, in particular in liquid solutions, the properties of drug molecules are significantly influenced by solvent molecules. Therefore, it is necessary to investigate the behavior of drug molecules in different solvents.

Solvent effects on the thermodynamics and kinetics of chemical and biological phenomena attract continuously increasing interest. It was said that the solvent effects can be split into two components: one is a perturbation of the UV spectrum (direct effect) and another is a modification of the ground-state geometry (indirect effect) (Preat et al., 2006). Much of what is known about the energetics involved comes from electronic spectroscopy, where frequency shifts between gas and solution phase, or among different solvents, serve to probe differences between the solvation of two electronic states. Recent advance in quantum calculation techniques are making ab initio calculations possible on larger size systems, thus ab initio procedures could provide reliable treatments of solute–solvent interactions, which makes it possible to describe chemical processes in solutions using theoretical methods (Wong et al., 1992; Foresman et al., 1996; Barone and Cossi, 1998). Meanwhile, advanced quantum chemical approach makes it available for a best understanding of the nature of both the ground and the excited states involved in the electronic absorption and its tuning by environmental effects.

Excited states are directly involved in the primary steps of the light absorption and charge transfer. Understanding of the excited states and of how their characteristics depend on the chemical environment (solvent, ligands) is of great interest for technological applications. Study of excited state molecular properties may be highly valuable as it may help explain their structure–property relationships under electronic excitation. The knowledge about precise electronic characteristic of pharmaceutical molecules such as a change of charge distributions in molecules following their electronic excitation can be helpful to determine the interactions between the receptors and the ligands as well as to understand the molecular mechanism of biological activities.

There is currently a great interest in extending density functional theory (DFT) to excited electronic states, the time dependent DFT (TDDFT) (Casda et al., 1998; Stratmann et al., 1998; Cossi and

* Corresponding author at: Key Laboratory for Nanomaterials, Ministry of Education, Research Center of the Ministry of Education for High Gravity Engineering and Technology Beijing University of Chemical Technology, Beijing 100029, PR China. Tel.: +86 10 64446466; fax: +86 10 64423474.
E-mail address: chenjf@mail.buct.edu.cn (J.-F. Chen).

0378-5173/$ – see front matter © 2008 Published by Elsevier B.V.
doi:10.1016/j.ijpharm.2008.03.033

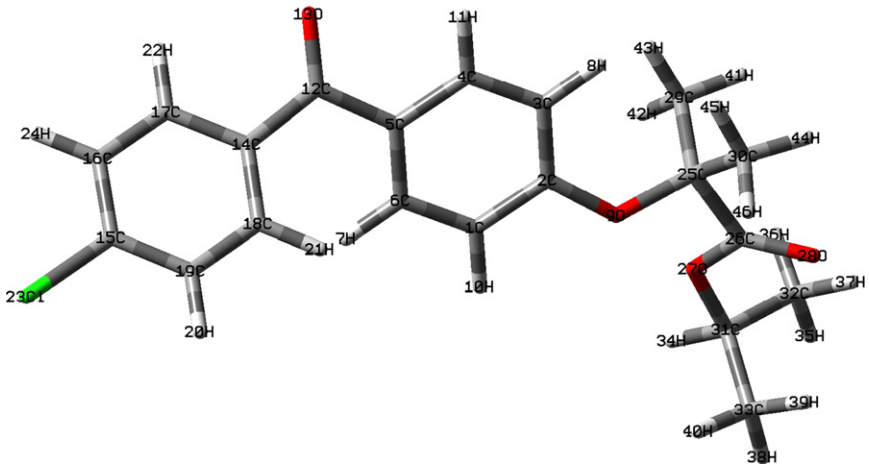

Fig. 1. Optimized structure of fenofibrate determined at the B3LYP/6-31G* level.

Barone, 2001) approach offers a rigorous route to the calculation of vertical electronic excitation spectra (Wan et al., 2004; Bellete et al., 2005), which is proved to be a powerful and effective computational tool for the study of ground and excited state properties by comparison to the available experimental data (Guillemoles et al., 2002; Cave et al., 2002). The theoretical study of the electronic excitations of molecules can provide a sophisticated understanding and the assignments of spectral features. Up to now, to our knowledge, very little work has been reported to provide reliable predictions of UV spectra of drug molecules in solvent-phases.

In this work, our aim is to investigate the solvent effects on molecular geometry and electronic structure of fenofibrate, and survey the solvent effects on the singlet vertical excited states of fenofibrate. To hit this target, we use TDDFT combining with polarizable continuum model (PCM) method (Cossi et al., 1996; Aguilar et al., 1993; Cossi et al., 1998) to obtain λ_{max} and compare with the experimental UV absorption spectra of fenofibrate

2. Experimental and computational details

Fenofibrate is virtually insoluble in water, thus the UV–vis spectra was obtained in tetrahydrofuran (THF), ethanol (EtOH) and dimethylsulfoxide (DMSO) solutions which performed on Shimadzu UV-2501PC.

All quantum calculations were carried out using the B3LYP flavor of density functional theory. Geometry optimizations were performed at the B3LYP/6-31G(d), B3LYP/6-311G(d,p) and B3LYP/6-311++G(d,p) levels in gas phase. Consequently, PCM is used for evaluating the bulk solvent effects, in which one divides the problem into a solute part (fenofibrate) lying inside a cavity and a solvent part (in our case, THF, EtOH, DMSO and water) represented as a structureless material, characterized by its dielectric constant as well as other parameters (Preat et al., 2006). For gas phase geometry vibrational frequencies were calculated analytically to ensure it to be a true local minimum (no imaginary frequencies). The effect of solute–solvent interaction was taken into account by PCM method.

TDDFT was used to study the vertical electronic excitation processes. Calculations were carried out at the optimized structures in gas phase and in THF, EtOHl and DMSO solutions combined with the PCM method. To investigated the basis set effects, comparison was also performed at the B3LYP/6-31G(d), B3LYP/6-311G(d,p) and B3LYP/6-311++G(d,p) levels for the excited states of fenofibrate in the gas phase and solutions.

All calculations were performed using Gaussian 03 package on the Intel Pentium IV PC.

3. Results and discussion

3.1. Geometrical structures

The results of the geometries optimization and the key data from the X-ray structure analysis on fenofibrate crystal (Henry et al., 2003) are summarized in Table 1. The optimized geometries (Fig. 1) are consistent with the experimental data, the average differences between the experimental and calculated geometries are 0.0123 Å in bond length and 1.52° in angle. To compare the effect of basis set, we carried out geometry optimizations at B3LYP/6-31G(d), B3LYP/6-311G(d,p) and B3LYP/6-311++G(d,p) levels in gas phase. The optimized geometries are relatively unaffected by the basis set, the maximum deviation of bond length and bond angle is only 0.0008 Å and 0.1° respectively.

To see how the solvation will affect the geometry, we also performed the geometry optimization of fenofibrate using the PCM at B3LYP/6-31G(d) level. As shown in Table 1, solvation only slightly compacted the molecule, reoptimized geometry parameters in the dielectric continuum corresponding to the aqueous solution ($\varepsilon = 78.39$) leads to small changes by no more than 0.01 Å in bond lengths and 1° in angles, which means the introduction of a solvent reaction field has slight effect on the geometry of fenofibrate.

3.2. Energies and dipole moments

The calculated total molecular energies (E_T), solvent energies (E_S), frontier orbital energies and ground-state dipole moments of fenofibrate in vacuo and in solutions by B3LYP/6-31G(d) are listed in Table 2. With the increase of solvent dielectric constant (ε_r), the total molecular energies and the energy gap (ΔE) between the highest occupied molecular orbital (HOMO) and the lowest unoccupied molecular orbital (LUMO) slightly decrease while solvent energies (E_S) and dipole moments enhance. UV absorption wavelength versus the ΔE, so that the wavelength is predicted increased with the increase of ε_r. Solvent effects improve the charge delocalized in the molecules, therefore, induce the dipole moments raised, furthermore, solvent energies show correlation with the dielectric constant or dipole moment. Ground-state dipole moment is an important factor in measuring solvent effect, a large ground-state dipole moment gives rise to a strong solvent polarity effects (Masternak et al., 2005). Meanwhile, the ground-state dipole moment caused the reorientation of solvent molecules to produce a large reaction field, in turn results in a shift between the energies of the ground and excited state, which induce the shift

Table 1
Optimized geometries for fenofibrate

	6-311++G(d,p)	6-311G(d,p)	6-31G(d)					
	Gas $\varepsilon_r = 1.0$	Gas $\varepsilon_r = 1.0$	Gas $\varepsilon_r = 1.0$	THF $\varepsilon_r = 7.58$	EtOH $\varepsilon_r = 24.55$	DMSO $\varepsilon_r = 46.7$	Water $\varepsilon_r = 78.39$	X-ray
$R(Cl_{23}–C_{15})$	1.7562	1.7563	1.7563	1.7606	1.7617	1.7620	1.7621	1.7397
$R(O_9–C_2)$	1.3599	1.3599	1.3598	1.3543	1.3528	1.3524	1.3523	1.3603
$R(O_9–C_{25})$	1.4478	1.4477	1.4475	1.4544	1.4561	1.4565	1.4567	1.4362
$R(O_{27}–C_{26})$	1.3378	1.3378	1.3370	1.3357	1.3352	1.3350	1.3350	1.3376
$R(O_{27}–C_{31})$	1.4677	1.4675	1.4677	1.4720	1.4732	1.4735	1.4736	1.4631
$R(O_{13}–C_{12})$	1.2275	1.2275	1.2275	1.2292	1.2295	1.2296	1.2297	1.2275
$R(O_{28}–C_{26})$	1.2141	1.2140	1.2140	1.2123	1.2122	1.2122	1.2122	1.2071
$R(C_{25}–C_{26})$	1.5534	1.5533	1.5533	1.5554	1.5557	1.5558	1.5559	1.5517
$\angle(C_2O_9C_{25})$	125.76	125.74	125.66	126.25	126.28	126.29	126.30	121.03
$\angle(C_{26}O_{27}C_{31})$	120.39	120.39	120.38	120.53	120.53	120.53	120.53	117.62
$\angle(C_5O_{13}C_{12})$	120.33	120.33	120.33	120.95	121.10	121.14	121.16	119.93
$\angle(C_5C_{12}C_{14})$	120.64	120.64	120.64	120.61	120.62	120.63	120.63	120.59
$\angle(C_1O_9C_2)$	114.58	114.56	114.06	113.86	113.89	113.91	113.91	114.29
$\angle(C_{25}O_{26}O_{28})$	123.00	122.99	122.99	122.97	122.98	122.88	122.87	122.90
$\angle(C_{25}O_{27}C_{26})$	111.25	111.23	111.17	110.80	110.79	110.79	110.79	112.08
$\angle(C_{25}O_9C_{26})$	103.31	103.38	103.11	102.08	102.01	102.00	101.99	111.82

Table 2
Calculated energies, dipole moments and frontier orbital energies

	Gas phase $\varepsilon_r = 1.0$	THF $\varepsilon_r = 7.58$	EtOH $\varepsilon_r = 24.55$	DMSO $\varepsilon_r = 46.7$	Water $\varepsilon_r = 78.39$
E_{total} (Hartree)	−1535.8822546	−1535.8836588	−1535.8840301	−1535.8841219	−1535.8841649
E_s (kJ mol^{-1})		3.687	4.662	4.903	5.015
E_{HOMO} (eV)	−0.22967	−0.22960	−0.22967	−0.022969	−0.22969
E_{LUMO} (eV)	−0.06320	−0.07112	−0.07328	−0.07382	−0.07407
ΔE (eV)	0.16647	0.15848	0.15639	0.15587	0.15562
μ (D)	3.9192	4.5455	4.7550	4.8046	4.8653

of UV absorption wavelength. From Table 2, we can see the dipole moments of fenofibrate varies just from 3.92 0D to 4.87 D in going from the $\varepsilon_r = 1$ to $\varepsilon_r = 78.39$, which also demonstrate that the solvent effects on fenofibrate are limited.

3.3. Mulliken atomic charges

The charge distributions of dipolar compounds are often altered significantly in the presence of a solvent reaction field. We have examined the Mulliken atomic charges both in gas phase and in solutions. The results are shown in Table 3. The difference on charge distributions is in accord with the changes in dipole moments and molecular geometries. As expected, the charge distributions are slightly influenced by a dielectric medium. A large degree of changes is predicted with the increasing of dielectric constant. The maximum change in charge occurs at carbonyl oxygen O_{13}, increasing in going from gas phase to aqueous solution just by 0.0098 e.

Table 3
Calculated Mulliken atomic charges in the S_0 states of fenofibrate

Atom	Gas	THF	EtOH	DMSO	Water
C(1)	−0.185910	−0.186332	−0.186274	−0.186256	−0.186252
C(2)	0.399005	0.405818	0.407086	0.407391	0.407543
C(3)	−0.192362	−0.191661	−0.191166	−0.191016	−0.190978
C(4)	−0.164661	−0.164866	−0.164854	−0.164853	−0.164849
C(5)	0.070254	0.069428	0.069448	0.069456	0.069456
C(6)	−0.181537	−0.182306	−0.182767	−0.182890	−0.182935
O(9)	−0.555750	−0.552070	−0.551035	−0.550761	−0.550638
C(12)	0.319110	0.317091	0.316573	0.316439	0.316374
O(13)	−0.472589	−0.479929	−0.481716	−0.482165	−0.482371
C(14)	0.073786	0.075547	0.075984	0.076100	0.076150
C(15)	−0.059440	−0.058753	−0.058542	−0.058488	−0.058463
C(16)	−0.134926	−0.135448	−0.135572	−0.135604	−0.135618
C(17)	−0.148012	−0.147865	−0.147830	−0.147816	−0.147814
C(18)	−0.173992	−0.173540	−0.173459	−0.173432	−0.173421
C(19)	−0.137456	−0.137407	−0.137391	−0.137389	−0.137386
Cl(23)	−0.015506	−0.031340	−0.035728	−0.036835	−0.037350
C(25)	0.241827	0.238073	0.236670	0.236308	0.236150
C(26)	0.641434	0.645712	0.646490	0.646668	0.646758
O(27)	−0.472829	−0.476692	−0.477430	−0.477591	−0.477684
O(28)	−0.488203	−0.481523	−0.480247	−0.479963	−0.479805
C(29)	−0.487180	−0.484403	−0.484368	−0.484346	−0.484362
C(30)	−0.462337	−0.462963	−0.463177	−0.463265	−0.463275
C(31)	0.138021	0.134015	0.132891	0.132616	0.132488
C(32)	−0.469389	−0.470233	−0.470505	−0.470573	−0.470605
C(33)	−0.469628	−0.469297	−0.469212	−0.469191	−0.469180

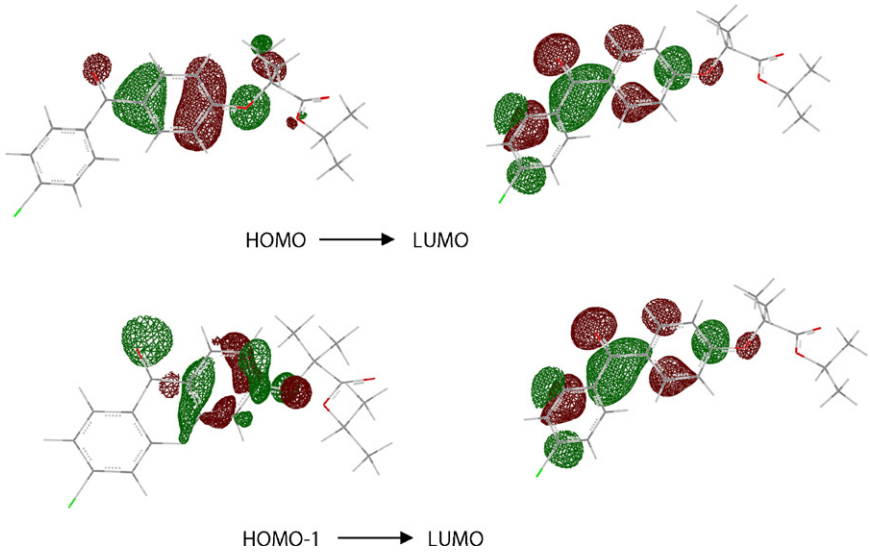

Fig. 2. Molecular orbitals for the two electronic transitions of fenofibrate in gas phase from the DFT calculations.

3.4. Electronic spectrum

The molecule of fenofibrate consists of 421 molecular orbitals, the features of the HOMO and the LUMO can be seen in Fig. 2, both the HOMO and LUMO mainly present π symmetry. The HOMO is dominately composed of p orbitals of the C atoms on one phenyl ring and p orbitals of carbonyl oxygen O_{13} atom, in contrast, the LUMO is essentially π^* antibonding orbitals of C atoms localized on two phenyl rings combined with antibonding orbitals of carbonyl carbon atom C_{12} as well as carbonyl oxygen O_{13} atom.

The application of the TDDFT method for estimates of excited state parameters for fairly large molecules is becoming very popular. The active space of TDDFT calculation consists of the complete molecular orbital space. TDDFT calculations for fenofibrate in the gas phase have captured the essence of the experimental UV spectra in solutions, that is, all the active transitions can be described as the $\pi \rightarrow \pi^*$ singlet excitation, the dominated contributions to the maximum absorption come from the HOMO → LUMO and HOMO-1 → LUMO transition (see Fig. 2), taking up 66% and 34% respectively, in gas phase.

To investigate the basis set effects on the excitation calculations, we have selected the 6-31G(d), 6-311G(d,p) and 6-311++G(d,p) basis sets (BS) with the B3LYP functional for the TDDFT calculation. In Table 4 the TDDFT-PCM results and the experimental spectra of fenofibrate in solutions are compared. For solvated fenofibrate, there is a nice agreement between experimental and theoretical λ_{max}. From Table 4, we see that TDDFT results slightly depend on the size of basis sets for the prediction of λ_{max}, smaller BS yielding too small λ_{max} in nm. These three basis sets virtually give similar results with difference of less than 7 nm. Among the three basis sets, the results of B3LYP/6-311++G(d,p) are very close to the experimentals, the λ_{max} are 285 nm with oscillator strength of 0.49 in THF and 286 nm with oscillator strength of 0.48 in ethanol as well as 287 nm with oscillator strength of 0.49 in DMSO, respectively. In going from the gas phase to solutions, we can observe a solvatochromic shift in band position, the band is indeed shifted to longer wavelength. This shift improves the agreement with the experimental data.

Table 4
Absorption spectrum of fenofibrate with TDDFT calculations

Solvent	λ_{max} (nm)			
	6-31G(d)	6-311G(d,p)	6-311++G(d,p)	Experimental
Vapor	272	275	278	
THF	279	281	285	284
EtOH	281	282	286	285
DMSO	281	283	287	288

4. Conclusion

The molecular geometry and the UV spectra of fenofibrate in solutions have been investigated by using TDDFT approach at various levels, miming the solvents with PCM method. We conclude that the solvent effects on the molecular structure of fenofibrate are not obvious and the singlet vertical excitation energies of fenofibrate do not much depend on the size of basis sets. The computed results show TDDFT-PCM calculations lead to a very closer agreement with the experimental absorption spectra in solutions, which demonstrate the importance of consideration of the solvating effects in interpreting experimental absorption spectra in solution and TDDFT is a powerful and effective computational tool for the study of ground and excited state properties.

Acknowledgment

This work was supported by National “863” Program of China (No. 2006AA03A205).

References

Aguilar, M.A., Olivares, F.J., Tomasi, J., 1993. Nonequilibrium solvation: an ab initio quantum-mechanical method in the continuum cavity model approximation. J. Chem. Phys. 98, 7375–7384.
Barone, V., Cossi, M., 1998. Quantum calculation of molecular energies and energy gradients in solution by a conducor solvent mode. J. Phys. Chem. A 102, 1995–2001.
Bellete, M., Morin, J.F., Leclerc, M., Durocher, G., 2005. A theoretical, spectroscopic, and photophysical study of 2.7-carbazolenevinylene-based conjugated derivatives. J. Phys. Chem. A 109, 6953–6959.
Casda, M.E., Jamorski, C., Casida, K.C., Salahub, D.R., 1998. Molecular excitation energies to high-lying bound states from time-dependent density-functional response theory: characterization and correction of the time-dependent local density approximation ionization threshold. J. Chem. Phys. 108, 4439–4449.
Cave, R.J., Edward, W., Castner Jr., 2002. Time-dependent density functional theory investigation of the ground and excited states of coumatins 102, 152, 153 and 343. J. Phys. Chem. A 106, 12117–12123.
Chong, P.H., Bachenheimer, B.S., 2000. Current, new and future treatments in dyslipidaemia and atherosclerosis. Drugs 60, 55–93.

Cossi, M., Barone, V., 2001. Time-dependent density functional theory for molecules in liquid solutions. J. Chem. Phys. 115, 4708–4717.
Cossi, M., Barone, V., Cammi, R., Tomasi, J., 1996. Ab initio study of solvated molecules: a new implementation of the polarizable continuum model. Chem. Phys. Lett. 255, 327–335.
Cossi, M., Barone, V., Mennucci, B., Tomasi, J., 1998. Ab initio study of ionic solutions by a polarizable continuum dielectric model. Chem. Phys Lett. 286, 253–260.
Foresman, J.B., Keith, T.A., Wiberg, K.B., Snoonian, J., Frisch, M.J., 1996. Solvent effects. 5. Influence of cavity shape, truncation of electrostatics, and electron correlation on ab initio reaction field calculations. J. Phys. Chem. 100, 16098–16104.
Guillemoles, J.-F., Barone, V., Joubert, L., Admo, C., 2002. A theoretical investigation of the ground and excited states of selected Ru and Os polypyridyl molecular dyes. J. Phys. Chem. A 106, 11354–11360.
Henry, R.F., Zhang, G.Z., Gao, Y., Buc kner, I.S., 2003. Fenofibrate Acta Cryst. E59, o699–o700.
Masternak., A., Wenska, G., Milecki, J., Skalski, B., Franzen, S., 2005. Solvatochromism of a novel betaine dye derived from purine. J. Phys. Chem. 109, 759–766.
Milionis, H.J., Elisaf, M.S., Mikhailidis, D.P., 2000. Treatment of dyslipidaemias in patients with established vascular disease: a revival of the fibrates. Curr. Med. Res. Opin. 16, 21–32.
Preat, J., Jacquemin, D., walthelet, V., Andre, J.M., Perpete, E.A., 2006. TD-DFT investigation of the UV spectra of pyranone derivatives. J. Phys. Chem. A 110, 8144–8150.
Shi, G.Q., Dropinski, J.F., Zhang, Y., Santini, C., et al., 2005. Novel 2 3-dihydrobenzofuran-2-carboxylic acids: highly potent and subtype-selective PPARαagonists with potent hypolipidemic activity. J. Med. Chem. 48, 5589–5599.
Stratmann, R.E., Scuseria, G.E., Frisch, M.J., 1998. An efficient implementation of time-dependent density-functional theory for the calculation of excitation energies of large molecules. J. Chem. Phys. 109, 8218–8224.
Wan, J., Ren, Y.L., Wu, J.M., Xu, X., 2004. Time-Dependent density functional theory investigation of electronic excited states of tetraoxaporphyrin dication and porphycene. J. Phys. Chem. A 108, 9453–9460.
Wong, M.W., Frisch, M.J., Wiberg, K.B., 1992. Solvent effects 3 Tautomeric equilibria of formamide and 2-pyridonge in the gas phase and solution. An ab initio SCRF study. J. Am. Chem. Soc. 114, 1645–1652.